

**ESR observations of paramagnetic centers in intrinsic hydrogenated microcrystalline silicon**

M. M. de Lima, Jr.\* and P. C. Taylor

*Department of Physics, University of Utah, Salt Lake City, Utah 84112*

S. Morrison and A. LeGeune

*MV Systems, Golden, Colorado 80401*

F. C. Marques

*Departamento de Física Aplicada, Instituto de Física "Gleb Wataghin," Universidade Estadual de Campinas-Unicamp, Campinas-São Paulo, Brazil*

(Received: 27 August 2001; revised manuscript received 4 March 2002; published 18 June 2002)

Paramagnetic centers in hydrogenated microcrystalline silicon,  $\mu c$ -Si:H have been studied using dark and light-induced electron-spin resonance (ESR). In dark ESR measurements only one center is observed. The  $g$  values obtained empirically from powder-pattern line-shape simulations are  $g_{\parallel} = 2.0096$  and  $g_{\perp} = 2.0031$ . We suggest that this center may be due to defects in the crystalline phase. During illumination at low temperatures, an additional ESR signal appears. This signal is best described by two powder patterns indicating the presence of two centers. One center is asymmetric ( $g_{\parallel} = 1.999$ ,  $g_{\perp} = 1.996$ ), while the other is characterized by large, unresolved broadening such that unique  $g$  values cannot be obtained. The average  $g$  value for this center is 1.998. The light-induced signal, which we interpret as coming from carriers trapped in the band tails at the crystalline grain boundaries, remains for at least several minutes after the light is turned off. Although the time scales of the decay curves are very different for two samples prepared by different techniques, both decays can be fitted using the assumption of recombination due to distant pairs of electrons and holes trapped in localized band-tail states.

DOI: 10.1103/PhysRevB.65.235324

PACS number(s): 61.72.Ji, 71.23.-k, 61.43.-j, 76.30.-v

**I. INTRODUCTION**

Over the past few years, hydrogenated microcrystalline silicon,  $\mu c$ -Si:H, has been studied mainly because of its importance for potential applications in flat panel displays and photovoltaic devices. The study of defects in  $\mu c$ -Si:H is particularly important, because defects limit most of the transport properties. A very important tool to investigate these defects is electron-spin resonance (ESR) spectroscopy. Systematic studies of the paramagnetic centers in  $\mu c$ -Si:H were first presented in 1994.<sup>1</sup> Since the majority of the defects have  $g$  values near to that of free electrons, where  $g = 2.0023$ , a unique interpretation of the different centers is difficult and remains controversial. In this work, we provide additional interpretations for some of the ESR signals previously observed in  $\mu c$ -Si:H.

Hydrogenated microcrystalline silicon as prepared by plasma-enhanced chemical vapor deposition (PECVD) of silane ( $\text{SiH}_4$ ) and hydrogen ( $\text{H}_2$ ) is a very inhomogeneous material. Such films typically consist of individual grains of crystalline silicon of  $\approx 10$ – $20$  nm, which aggregate into larger multigrain structures that can be as large as  $\sim 1$   $\mu\text{m}$  depending on the processing conditions and the thicknesses of the films. In addition, there is always a small component of hydrogenated amorphous silicon ( $a$ -Si:H) that exists primarily between the aggregated grains. Usually, there is no evidence for a preferred orientation for the individual grains,<sup>2</sup> although recently films with grains exhibiting at least partial  $\langle 220 \rangle$  ordering have been reported.<sup>2</sup>

**II. EXPERIMENT**

Two microcrystalline samples have been studied in this work. Sample 1 was prepared by PECVD using a 70-MHz

plasma excitation frequency and 3%  $\text{SiH}_4$  in an  $\text{H}_2$  atmosphere. This sample was deposited on an aluminum foil and removed using dilute HCl, resulting in 39 mg of powder. Further details concerning the preparation conditions for this sample can be found elsewhere.<sup>3</sup> Sample 2 was prepared using a 60-W pulsed-plasma reactor and 1%  $\text{SiH}_4$  in an  $\text{H}_2$  atmosphere. Four films were deposited in the same run on quartz substrates ( $4 \times 20$  mm<sup>2</sup>). Raman spectroscopy shows a crystalline fraction higher than 70% for both samples. Above this crystalline fraction, the amorphous peak is too small for an accurate determination. Atomic force microscopy (AFM) measurements<sup>4</sup> show that sample 2 has very large aggregated grains ( $\sim 0.3$   $\mu\text{m}$ ). These films also exhibit very good electrical properties, such as high photoconductivity, and they have been used to make solar cell devices with  $\sim 4\%$  efficiency.<sup>5</sup>

The ESR experiments were performed using a standard Bruker spectrometer with an X-band cavity (at  $\sim 9.5$  GHz). Dark ESR experiments were run at 10 K and room temperature at microwave powers, which avoided saturation of the signal. The optically induced studies employed a He-Ne laser (at 632.8 nm) with  $\sim 1$  mW power. Both dark and light-induced measurements were made at a magnetic-field modulation amplitude of 0.1 mT and a modulation frequency of 100 kHz.

**III. RESULTS**

Figure 1 shows the dark ESR signal for sample 1 obtained at room temperature using 100  $\mu\text{W}$  of microwave power. The asymmetric line shape can be simulated (dotted line) assuming a powder pattern of a single center with  $g_{\parallel}$

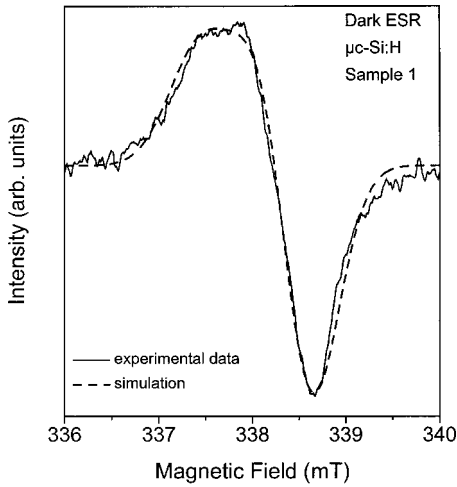


FIG. 1. Dark ESR signal from  $\mu c$ -Si:H (sample 1) taken at room temperature using a microwave power of  $100 \mu\text{W}$  and a modulation amplitude of  $0.1 \text{ mT}$  at a microwave frequency of  $9.490 \text{ GHz}$ . The dotted line is a simulation assuming a powder pattern with  $g_{\parallel} = 2.009$  and  $g_{\perp} = 2.003$  and Gaussian broadening of  $0.3 \text{ mT}$ .

$= 2.0096$ ,  $g_{\perp} = 2.0031$ , and a Gaussian broadening of  $0.32 \text{ mT}$ . The spin density was estimated to be about  $1 \times 10^{17} \text{ cm}^{-3}$ . No other dark ESR signal was observed, even at low temperatures. The intensity of the dark ESR signal multiplied by the temperature (in order to adjust for spin state population differences produced by changes in temperature) as a function of microwave power is shown in Fig. 2 for  $10 \text{ K}$  and room temperature. The straight line is a linear regression, whose slope is  $0.49 \pm 0.01$ . For an unsaturated signal the slope should be  $0.5$ . At room temperature the signal is not saturated until  $\approx 1 \text{ mW}$  of microwave power. At  $10 \text{ K}$ , on the other hand, the signal is always saturated, even at very low microwave power, such as  $1 \mu\text{W}$ . The saturation remains for temperatures as high as  $150 \text{ K}$ . As compared with the unsaturated signal at room temperature, the signal at

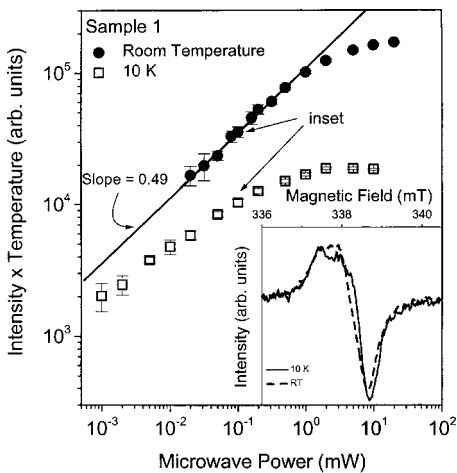


FIG. 2. ESR intensity multiplied by temperature as a function of microwave power at  $10 \text{ K}$  and room temperature. The dotted line has a slope  $0.49 \pm 0.01$  and represents unsaturated behavior. The arrows indicate the spectra shown in the inset. The signals are normalized to display the same unsaturated intensity.

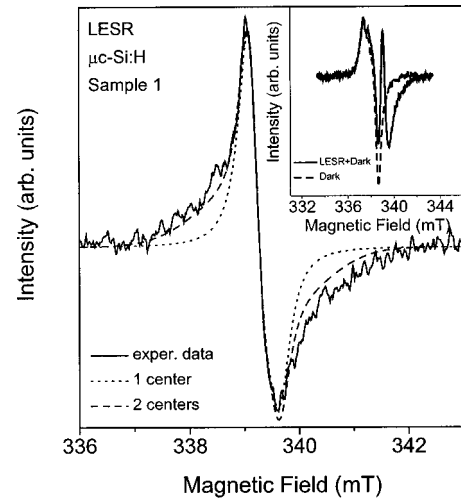


FIG. 3. LESR signal of  $\mu c$ -Si:H (sample 1) taken at  $15 \text{ K}$  using a microwave power of  $10 \text{ mW}$  and a modulation amplitude of  $0.1 \text{ mT}$  at a microwave frequency of  $9.489 \text{ GHz}$ . The dotted line is the result of a simulation using a powder pattern with  $g_{\parallel} = 1.999$  and  $g_{\perp} = 1.996$  and Lorentzian broadening of  $0.3 \text{ mT}$ . The dashed line represents a simulation in which a second center with  $g = 1.998$  is also included with an equal concentration. The inset shows both the dark signal and the (LESR+dark) signal.

$10 \text{ K}$  has a modified line shape, as one can see in the inset to Fig. 2. The dark signal in sample 2 was not studied in detail because it was barely detectable.

Sample 2, which consists of four films on quartz substrates, contains much less material, and in addition the dark spin density is much smaller ( $\leq 10^{16} \text{ spins/cm}^3$ ) than that in sample 1. Finally, because sample 2 is on a quartz substrate, there exists an  $e'$  signal on the substrate that is created during the film deposition.<sup>6</sup> This signal partially overlaps the dark spin signal from the  $\mu c$ -Si:H.

Figure 3 shows the light-induced signal in sample 1 with the dark signal removed by subtraction. The dark signal and the dark-plus-light-induced signal are shown in the inset to Fig. 3 by the dashed and solid curves, respectively. Two different simulations are shown: (1) a single center consisting of an axially symmetric powder pattern with  $g_{\parallel} = 1.999$  and  $g_{\perp} = 1.996$  convoluted with Lorentzian broadening of  $0.3 \text{ mT}$  (dotted line); and (2) two centers consisting of the previous center and a center with a  $g$  tensor whose symmetric component is  $g = 1.998$  convoluted with Gaussian broadening of  $0.8 \text{ mT}$  (dashed line). The  $g$  tensor of the second center is assumed to be symmetric for simplicity, since the large Gaussian broadening masks any anisotropies in  $g$  value. In addition, the intensities of these two centers are assumed to be the same. Although the first simulation very well describes the central portion of the experimental derivative spectrum, the wings on both sides are not. The major difficulty is the superposition of a sharp central derivative feature with broad wings. The powder pattern of a single center cannot easily account for both the features. On the other hand, adding a second center produces a much better fit. As mentioned above, the choice of a symmetric  $g$  tensor for the second center is a convenience, since the broadening hides

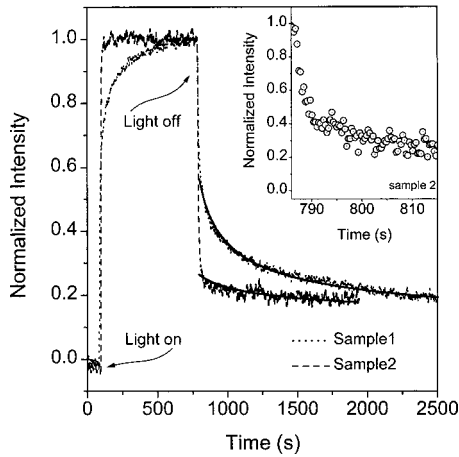


FIG. 4. Growth and decay curves for the LESR center for two different samples. Both signal intensities are normalized to 1 just before the light is turned off. The solid lines are fits using a distant-pair recombination model discussed in the text.

any asymmetry in the  $g$  values, and the 1:1 ratio between the two centers was chosen for simplicity but seems roughly correct.

Light-induced ESR (LESR) measurements were also performed on sample 2 and, within the noise, the result was identical to that displayed in Fig. 3. The LESR signal at 10 K did not show saturation with respect to microwave power even at 30 mW. This result is probably due to a spin-lattice-relaxation mechanism that is enhanced by interactions with the relatively larger density of optically excited spins. With the light intensity used, the light-induced effect was observed at temperatures as high as 70 K. However, the photoexcited spin density is reduced noticeably for temperatures higher than  $\sim 40$  K. As the inset to Fig. 3 shows, there is no contribution to the LESR from the lineshape associated with the dark ESR. This result holds independent of the temperature. In addition, there is no change in the LESR line shape as a function of temperature, although the line is barely detectable at 70 K.

When the illumination is discontinued, the intensity of the light-induced resonance decreases. However, the signal does not go to zero, remaining around 20% of the original intensity for at least several minutes after the light is turned off. Figure 4, shows the growth and decay curves of the light-induced center for samples 1 and 2 at 15 K. Although, the time scales are completely different (Sample 2, which has better electronic properties, exhibits a much faster decay.), the spectra for both samples can be fitted using a model discussed by Yan *et al.*<sup>7</sup> for distant-pair recombination via tunneling between localized states (solid curves in Fig. 4).

#### IV. DISCUSSION

Two major signals are usually observed in the dark ESR of intrinsic, hydrogenated microcrystalline silicon. One signal, often associated with silicon dangling bonds, has a zero crossing  $g$  value for the ESR derivative spectrum around 2.005 (close to the  $a$ -Si:H dangling bond value).<sup>8</sup> The other signal, which appears in low electronic quality samples or

TABLE I.  $g$  values for relevant defects in crystalline and amorphous silicon solids: dangling bonds, DB; Si dangling bonds at the  $\text{SiO}_2/c$ -Si interface,  $P_b$ ; and Si vacancy,  $V$ .

Defect	$g_{\parallel}$	$g_{\perp}$	Reference
DB in $a$ -Si:H	2.0039	2.0065	14
$P_b$ in $c$ -Si	2.0011	2.0080	15
	2.0016	2.0090	16
$V^-$ in $c$ -Si	2.0151	2.0038, 2.0028 <sup>a</sup>	17
$V^+$ in $c$ -Si	2.0087	1.9989	17
$\mu c$ -Si:H	2.0096	2.0031	This work

<sup>a</sup>In these case  $g_2$  is slightly different from  $g_3$ , however this result is not very far from axial symmetry.

under illumination, has a  $g$  value of 1.998. The interpretation of these centers is still a matter of debate.

Several authors have attributed the asymmetry of the  $g = 2.005$  signal to the presence of two different centers.<sup>9–13</sup> The first center is supposed to be a Si dangling bond with a  $g$  value of 2.0052. The second center ( $g = 2.0043$ ) was initially attributed to electrons trapped in the conduction band tails,<sup>9</sup> since its  $g$  value is very close to that observed in  $n$ -type  $a$ -Si:H (Ref. 10) and in intrinsic  $a$ -Si:H under illumination.<sup>11</sup> Another explanation of the second center is the presence of Si dangling bonds in an oxygen-rich environment.<sup>12</sup> More recently, Kondo, Yamasaki and Matsuda<sup>13</sup> have attributed the signal near 2.005 and its structure to the presence of  $P_b$  centers with  $g_{\parallel} = 2.0022$  and  $g_{\perp} = 2.0078$ . However, this interpretation is considered by some to be ambiguous because the interference of an ESR signal from the amorphous phase results in many adjustable parameters in the simulated spectrum.

One reason for controversy in the interpretation of the dark ESR spectrum is that microcrystalline silicon is a material that shows a very complex morphological structure. In addition to the (usually) randomly oriented crystalline grains, an amorphous phase, boundaries between the amorphous and crystalline phases, and boundaries between different crystalline grains also occur. In principle, the paramagnetic defects in this material could occur in any of these regions making their identification difficult. The paramagnetic defects expected in the amorphous phase are the well-known silicon dangling bonds (DB defect), typically found in  $a$ -Si:H. If oxygen impurities collect at the boundaries, one might expect the presence of  $P_b$  centers that often appear at Si/SiO<sub>2</sub> interfaces. In addition, in the crystalline phase one might expect various paramagnetic point defects, such as charged vacancies, divacancies, and larger clusters of vacancies. Table I lists previously published  $g$  tensors for the following defects: the DB in  $a$ -Si:H,<sup>14</sup> the  $P_b$  center on surfaces of  $c$ -Si,<sup>15,16</sup> and the vacancy.<sup>17</sup>

The previous attribution of the dark ESR signal to Si dangling bonds<sup>1,9,18</sup> seems unlikely. First, the spin density measured is too high to be due only to the small amorphous fraction or to interfaces between crystalline and amorphous silicon. Due to the hydrogenation, most of the potential silicon dangling bonds will be passivated. Second, the silicon dangling bond in  $a$ -Si:H has  $g_{\parallel} < g_{\perp}$  which leads to an asym-

metry in the line shape opposite to that found in  $\mu c$ -Si:H. Similarly, the  $P_b$  center has the wrong asymmetry as compared with the result shown here. Conversely, the  $g$  values obtained for  $\mu c$ -Si:H in this work ( $g_{\parallel}=2.0096$  and  $g_{\perp}=2.0031$ ) are consistent with those reported for charged vacancies in crystalline silicon.

However, the attribution of the dark ESR signal to single, isolated vacancies is not straightforward, since they anneal out at temperatures well below room temperature ( $V^+ \sim 180$  and  $\sim 60$  K).<sup>17</sup> On the other hand, vacancies can combine to form more complex structures such as divacancies<sup>19</sup> or even larger vacancy clusters<sup>20</sup> with different binding energies and annealing temperatures. In crystalline silicon, these defects are usually created by bombardment, and their stability is strongly dependent on temperature.<sup>20,21,22</sup> For instance, the five-vacancy cluster in  $c$ -Si, which can be generated by neutron irradiation, is stable at room temperature.<sup>20</sup> Thus, since the  $\mu c$ -Si:H is produced under strong nonequilibrium conditions, it is plausible that the crystalline phase has a relatively high density of stable defects ( $1 \times 10^{17} \text{ cm}^{-3}$ ). Of course, a detailed identification of this dark ESR signal of  $\mu c$ -Si:H is very difficult, since there are many possible aggregates of vacancies. Further investigations are needed to refine the microscopic identification of this ESR signal in  $\mu c$ -Si:H.

Another important feature that may help to clarify the origin of the dark ESR signal is its saturation at very low microwave powers at low temperatures. Figure 2 shows clearly that at low temperatures the signal is always saturated because the 10 K data lie below the extrapolated room-temperature data at all microwave powers. This behavior is probably due to the presence of a distribution of relaxation times. Even though at low enough microwave power the difference between the intensities due to saturation is only a factor of 2—a factor that is tolerable for estimations of the spin density—the changes in the line shape cannot be ignored if one wants to determine properly the  $g$  values to compare with well-known centers. In addition, these changes in the line shape due to saturation cannot be used as an indication of the presence of two different centers, since another possible explanation for this behavior is the presence of an orientational dependence to the relaxation mechanism or to a change in the  $g$  values with temperature. For instance, in the above-mentioned five-vacancy cluster the changes in the  $g$  values with temperature will produce changes in the calculated, powder-pattern lineshapes.<sup>20</sup>

The identification of the LESR resonance with  $g$  around 1.998 is also unclear. Originally, this line was ascribed to free electrons in the conduction band, since its zero-crossing  $g$  value is almost the same as that for conduction electrons in crystalline silicon.<sup>1</sup> In addition, for  $n$ -doped  $\mu c$ -Si:H at low temperatures a resonance with the same  $g$  value as the LESR signal has been observed.<sup>9,18</sup> Finally, the same broadening in the line shape has been observed with increasing temperature as that found for conduction electrons in crystalline silicon.<sup>12</sup> However, others have attributed the LESR signal to electrons trapped in the localized, conduction-band-tail states.<sup>23–25</sup> This attribution is supported by a study of the photoconductivity and the density of LESR states as functions of the

generation rate.<sup>24,25</sup> These results can only be explained by means of localized carriers. Moreover, the asymmetric line shape is not consistent with free electrons in the conduction band. More recently, it has been proposed that in  $\mu c$ -Si:H doped with phosphorous the  $g=1.998$  signal is related to trapped electrons at low doping (and intrinsic) levels and to free electrons in the conduction band at high doping levels.<sup>26,27</sup>

At least for undoped samples, the LESR center seems to be related with photoexcited carriers trapped in the band tails. The presence of band-tail states is a natural consequence of disorder. Thus, in  $\mu c$ -Si:H, band-tail states could be related with: (1) strained bonds in the amorphous region; (2) defect states at the grain boundaries between crystalline grains or at crystalline/amorphous interfaces; and, in principle, (3) defects or impurities in the crystalline phase. The  $g$  values obtained for the LESR center in  $\mu c$ -Si:H are very different from those of optically excited carriers trapped in band-tail states in  $a$ -Si:H.<sup>11</sup> Also, the amorphous phase is only a small volume fraction of the film, and its contribution to the ESR and LESR is probably unimportant.

Of the two remaining possibilities, it is also unlikely that the LESR is due to band-tail states within the crystalline grains themselves. Although charged impurities, such as those that occur in highly doped and compensated Si, can produce band tails, the level of charged defects (assuming that the dark ESR is due to positively and negatively charged defects) is too small for significant band tailing to occur. Therefore, the LESR in  $\mu c$ -Si:H is probably due to carriers trapped in band-tail states at the grain boundaries between crystalline grains or at crystalline/amorphous interfaces.

Even though the possibility that the LESR signal is due to only a single center cannot be excluded, the results presented here are consistent with the presence of a second signal of equal intensity. Although the identification of these two signals with electrons and holes trapped at the crystalline interface is far from obvious (comparisons with  $a$ -Si:H are not very useful here), the sharpest line is probably due to electrons trapped in the conduction band tail, and the broad line is probably associated with holes trapped in the valence band tail. It is important to point out that ESR signals due to holes are not very often observed in crystalline silicon. However, if the photoexcited holes are trapped in localized, valence-band-tail states, which are not present in single crystals, their observation is plausible. In  $a$ -Si:H localized holes trapped in band-tail states are observed at temperatures exceeding 100 K.<sup>28</sup> This interpretation has the advantage that it provides a natural explanation for why no second line attributable to holes has been observed in intrinsic  $\mu c$ -Si:H under illumination.<sup>23,26,27</sup> The explanation is simply that the feature previously attributed to a single line is actually due to the sum of two.

Previous ESR studies<sup>9,18,29</sup> of doped  $\mu c$ -Si:H are generally consistent with the above explanation. In  $n$ -type  $\mu c$ -Si:H a sharp feature with  $g=1.998$  appears in the dark ESR, but in heavily boron-doped  $\mu c$ -Si:H only a very broad signal ( $\sim 50$  mT) with  $g \sim 2.1$  is observed. The line shape of this latter signal is probably heavily influenced by the presence of boron through an unresolved hyperfine interaction.<sup>29</sup> The absence of any signal clearly identified with holes in

valence-band-tail states in boron-doped  $\mu c$ -Si:H is not a surprise since the doping process in  $\mu c$ -Si:H is very different from that in  $a$ -Si:H. First, in microcrystalline silicon there is no autocompensation mechanism as there is in the amorphous material. Second, the doping efficiency is close to 1. Third, since any localized band-tail states in  $\mu c$ -Si:H probably exist at interfaces and have much narrower distributions in energy than in  $a$ -Si:H, it is probable that the holes are trapped at the relatively deep acceptors in the bulk and not in the band-tail states at the interfaces. In  $n$ -type  $\mu c$ -Si:H the shallower donors may, in fact, contribute electrons to the band-tail states at the interfaces. Because the line shape of the  $g=1.998$  resonance reported for heavily  $n$ -doped samples<sup>18,27</sup> is broader than the LESR in intrinsic films, one cannot test the possibility that in the  $n$ -doped case there is only a single center ascribed to electrons.

Finally, we discuss the decay of the LESR after the light was turned off for samples 1 and 2. Both curves are fitted using the model proposed by Yan *et al.*<sup>7</sup> for the LESR decay and growth curves due to distant-pair recombination via tunneling between localized states in  $a$ -Si:H. This model is based on the original ideas of Shoklovskii, Fritzsche, and Baranovskii<sup>30</sup> who demonstrate that, at low temperatures, the simultaneous diffusion and recombination of electron-hole pairs in amorphous solids does not depend on the form of the density of localized states. In other words, the decay is a universal property. The fact that the decay curves for the LESR in both microcrystalline samples can be fitted using this assumption is one more indication that the LESR is due

to carriers trapped in localized band-tail states. Since the two samples have different electronic properties, the large difference in the time scales of the decays is probably related to differences in the slopes of the band tails.

## V. CONCLUSION

The asymmetric, dark ESR signal in  $\mu c$ -Si:H, previously attributed to silicon dangling bonds, is probably related with defects in the crystalline grains. Using a powder-pattern simulation of the spectrum, the  $g$  values extracted for this center are  $g_{\parallel}=2.0096$  and  $g_{\perp}=2.0031$ . Another signal, which is observed only under illumination, is best described as due to two different centers. Electrons trapped in localized conduction-band-tail states and holes trapped in localized valence-band-tail states are the most likely centers. The center with  $g_{\parallel}=1.999$  and  $g_{\perp}=1.996$  is tentatively attributed to electrons, and the center with  $g=1.998$  is tentatively attributed to holes. The decay curves for the LESR provide additional support for this interpretation.

## ACKNOWLEDGMENTS

F. Finger is gratefully acknowledged for supplying sample 1. C. E. Inglesfield and J. L. Conlin are acknowledged for performing the AFM measurements. This work was supported by NREL under subcontracts Nos. ZAK-7-17619-16 and ADJ-2-30630-23 and by the Brazilian agency, FAPESP.

\*Present address: Universidade Estadual de Campinas, Unicamp, Instituto de Física "Gleb Wataghin," Departamento de Física Aplicada, Campinas-SP, Brazil, P.O. Box 6165, 13083-970.

<sup>1</sup>F. Finger, C. Malten, P. Hapke, R. Carius, R. Flückiger, and H. Wagner, *Philos. Mag. Lett.* **70**, 247 (1994).

<sup>2</sup>J. J. Gutierrez, C. E. Inglesfield, C. P. An, M. C. DeLong, P. C. Taylor, S. Morrison, and A. Madan, *Amorphous and Heterogeneous Silicon Based Films*, edited by M. Stutzman, J. B. Boyce, J. D. Cohen, R. W. Collins, and J. Hanna, Mater. Res. Soc. Symp. Proc. No. 664 (Materials Research Society, Pittsburgh, 2001), A3.4.1.

<sup>3</sup>P. Hari, P. C. Taylor, and F. Finger, in *Amorphous Silicon Technology 1996*, edited by M. Hack, E. A. Shiff, S. Wagner, R. Schropp, and A. Matsuda, Mater. Res. Soc. Symp. Proc. No. **420** (Materials Research Society, Pittsburgh, 1996), p. 491.

<sup>4</sup>C. E. Inglesfield and J. L. Conlin (unpublished).

<sup>5</sup>A. Madan (unpublished).

<sup>6</sup>See, for example, P. C. Taylor, in *Materials Issues in Applications of Amorphous Silicon Technology*, edited by D. Adler, A. Madan, and M. J. Thompson, Mater. Res. Soc. Symp. Proc. No. 49 (Materials Research Society, Pittsburgh, 1985), p. 61.

<sup>7</sup>B. Yan, N. A. Shultz, A. F. Efros, and P. C. Taylor, *Phys. Rev. Lett.* **84**, 4180 (2000).

<sup>8</sup>M. H. Brodsky and R. S. Title, *Phys. Rev. Lett.* **23**, 581 (1969).

<sup>9</sup>C. Malten, F. Finger, P. Hapke, T. Kulesa, C. Walker, R. Carius, R. Flückiger, and H. Wagner, in *Microcrystalline and Nanocryst-*

*talline Semiconductors*, edited by L. Brus, M. Hirose, R. W. Collins, F. Koch, and C. C. Tsai, Mater. Res. Soc. Symp. Proc. No. 358 (Materials Research Society, Pittsburgh, 1995), p. 757.

<sup>10</sup>R. A. Street, D. K. Biegelsen, and J. C. Knights, *Phys. Rev. B* **24**, 969 (1981).

<sup>11</sup>J. C. Knights, D. K. Biegelsen, and I. Solomon, *Solid State Commun.* **22**, 133 (1977).

<sup>12</sup>J. Muller, F. Finger, C. Malten, and H. Wagner, *J. Non-Cryst. Solids* **227–230**, 1026 (1998).

<sup>13</sup>M. Kondo, S. Yamasaki, and A. Matsuda, *J. Non-Cryst. Solids* **266–269**, 544 (2000).

<sup>14</sup>T. Umeda, S. Yamasaki, J. Isoya, and K. Tanaka, *Phys. Rev. B* **59**, 4849 (1999).

<sup>15</sup>K. L. Brower, *Appl. Phys. Lett.* **43**, 1111 (1983).

<sup>16</sup>W. E. Carlos, *Appl. Phys. Lett.* **50**, 1450 (1987).

<sup>17</sup>M. Sprenger, S. H. Muller, E. G. Sieverts, and C. A. J. Ammerlaan, *Phys. Rev. B* **35**, 1566 (1987).

<sup>18</sup>F. Finger, J. Müller, C. Malten, R. Carius, and H. Wagner, *J. Non-Cryst. Solids* **266–269**, 511 (2000).

<sup>19</sup>G. D. Watkins and J. W. Corbett, *Phys. Rev.* **138**, A543 (1965).

<sup>20</sup>Y. H. Lee and J. W. Corbett, *Phys. Rev. B* **8**, 2810 (1973).

<sup>21</sup>V. C. Venezia *et al.*, *Appl. Phys. Lett.* **79**, 1273 (2001).

<sup>22</sup>S. Chakravarthi and S. T. Dunham, *J. Appl. Phys.* **89**, 4758 (2001).

<sup>23</sup>M. Kondo, T. Nishimiya, K. Saito, and A. Matsuda, *J. Non-*

- Cryst. Solids **227–230**, 1031 (1998).
- <sup>24</sup>W. Fuhs, P. Kanschäat, and K. Lips, J. Vac. Sci. Technol. B **18**, 1792 (2000).
- <sup>25</sup>P. Kanschäat, K. Lips, and W. Fuhs, J. Non-Cryst. Solids **266–269**, 524 (2000).
- <sup>26</sup>F. Finger, J. Müller, C. Malten, and H. Wagner, Philos. Mag. B **77**, 805 (1998).
- <sup>27</sup>J. Müller, F. Finger, R. Carius, and H. Wagner, Phys. Rev. B **60**, 11 666 (1999).
- <sup>28</sup>R. A. Street and D. K. Biegelsen, and J. C. Knights, Phys. Rev. B **24**, 969 (1981).
- <sup>29</sup>C. Malten, F. Finger, J. Müller, and S. Yamasaki, in *Amorphous and Microcrystalline Silicon Technology–1998*, edited by S. Wagner, M. Hack, H. M. Branz, R. Schropp, and I. Shimizu, Mater. Res. Soc. Symp. Proc. No. 507 (Materials Research Society, Pittsburgh, 1999), p. 757.
- <sup>30</sup>B. I. Shklovskii, H. Fritzche, and S. D. Baranovskii, Phys. Rev. Lett. **62**, 2989 (1989).